Resource Allocation for Energy Harvesting-Powered D2D Communication Underlaying Cellular Networks

Ying Luo, Peilin Hong, Ruolin Su, and Kaiping Xue, *Senior Member, IEEE*

***Abstract*—Energy harvesting (EH)-powered wireless communications have attracted great attention from both industry and academia. However, the available energy, which relies on EH efficiency, will become another nonnegligible factor when we do research on EH-powered wireless communications. This paper studies the resource allocation problems in terms of spectrum and energy under EH-powered Device-to-Device (D2D) Communication underlaying Cellular Network (EH-DCCN). In this network, D2D pairs powered by EH are allowed to reuse the spectrum resources occupied by Cellular Users (CUs). To investigate the resource allocation problems, a sum-rate maximization problem of the whole cellular network with consideration of Quality of Service (QoS) and available energy constraints is formulated. The maximization problem is a nonconcave mixed-integer nonlinear programming (MINLP) problem, which has been proved to be NP-hard. To solve the problem, we first relax it with a concave lower bound on the original problem and then obtain the theoretical performance of the lower bound by Outer Approximation Algorithm. Moreover, a heuristic algorithm, an Energy-aware Space Matching approach (ESM), is proposed to acquire a suboptimal solution with low computational complexity. Finally, numerical simulation results indicate our considered resource allocation strategy is more effective than the strategy only based on channel state information under the EH-DCCN. Moreover, the performance in aspects of the sum rate and the matching probability shows that the ESM can approximately obtain the theoretical performance of the lower bound on the original problem under the scenarios with higher ratio of CU and EH-powered D2D numbers.**

***Index Terms*—D2D communications, energy harvesting, resource allocation, non-concave MINLP.**

I. Introduction

With the explosive growth of mobile devices and traffic loads, wireless networks are required to cope with the increasing traffic demands, while still providing desired Quality of Service (QoS). Thus, efficient wireless communication technologies are needed to be put forward to deal with this situation. Devive-to-Device (D2D) communication, which is deemed as one of key technologies of Long Term Evolution-Advanced (LTE-A) [1], enables devices to communicate directly with each other in close proximity via reusing the spectrum resources being assigned to Cellular Users (CUs) [2]. Obviously, D2D communication can alleviate spectrum deficiency, increase the capacity of cellular systems, decrease energy consumption etc.

Thus, it can be foreseen that a wide range of devices with D2D communication capability will be rapidly deployed in the near future. Such D2D communication devices may be the low-power devices (e.g., Machine-Type Devices (MTDs) [3]), which are typically equipped with fixed energy supplies, such as batteries with limited operation life [4]. Replacing batteries or charging power by a charger system for such devices is impractical and cost-prohibitive. Therefore, Energy Harvesting (EH), a technology that collects energy from environmental sources (e.g., solar, wind, radio frequency energy) and prolongs the lifetime of communications, has recently been considered as a possible alternative solution to overcome the bottleneck of energy constrained wireless networks [5] [6]. For instance, the D2D devices with solar panels may be the information distribution equipments for tourist attractions, a temporary large activity etc., and the mobile users (e.g., tourists, participants) can receive useful information (i.e., travel guide map, electronic flyers) from EH-powered D2D devices. Besides, EH technology is another way to provide green communication services [7]. Thus, EH-powered D2D communication not only has the potential ability to reach the system capacity of conventional D2D communications, but also can achieve green communications. Therefore, more and more researchers pay their attentions to the EH-powered D2D communication underlaying cellular networks, where D2D pairs powered by EH technique.

However, unlike the traditional D2D communication, the energy of ambient energy sources available to EH-powered D2D Users (DUs) is time-variant and often sporadic. This phenomenon will lead to a significant result: the energy will become another crucial impact factor to design the resource allocation policies in the aspects of spectrum resource assignment, power control, etc. Therefore, it is highly beneficial to do some resource management researches on EH-powered D2D communication underlaying cellular networks.

A. Related Works

Some related researches have been done on the EH-powered D2D communication. Ahmed *et al.* [6] modeled and analyzed EH-based D2D communication in cellular networks. They

Manuscript received May 15, 2017; accepted July 9, 2017. Date of publication July 14, 2017; date of current version November 10, 2017. This work was supported in part by the National Natural Science Foundation of China under Grants 61671420, 61672484, and 61379129, and the Fundamental Research Funds for the Central Universities. The review of this paper was coordinated by Dr. X. Huang. *(Corresponding author: Luo Ying.)*

The authors are with the Key Laboratory of Wireless-Optical Communications, School of Information Science and Technology, University of Science and Technology of China, Hefei 230026, China (e-mail: yingluo@mail.ustc.edu.cn; plhong@ustc.edu.cn; ruolinsu@mail.ustc.edu.cn; kpxue@ustc.edu.cn).

Color versions of one or more of the figures in this paper are available online at http://ieeexplore.ieee.org.

Digital Object Identifier 10.1109/TVT.2017.2727144

proposed two different spectrum access policies and evaluated the performance of the proposed policies with general path-loss exponent in terms of outage probability for D2D and cellular users. Howard *et al.* [8] proposed a D2D communication provided by EH Heterogeneous cellular Network (D2D-EHHN), where mobile User Equipment (UE) Relays (UERs) harvested energy from an Access Point (AP) and used the harvested energy to support D2D communication for enhancing communication reliability. In this model, the UER distribution was derived, and a transmission mode selection scheme was proposed. Authors of [9] considered sum-rate optimal power allocation policies for EH transmitters in a Gaussian interference channel. Yet the QoS requirement of each transmitter, which was mainly referred to transmission rate requirement, was not considered in the power allocation policies. Zhou *et al.* [10] investigated the energy-efficient power allocation problem under the non-causal knowledge of energy arrival. In addition, the various practical constraints of circuit power consumption, such as energy causality, battery capacity, were fully considered in the study.

The above research works were achieved with the assumption that the spectrum resources were already matched between cellular links and D2D links. The match indicated that the proper spectrum resource of CU link is allocated to D2D link based on Non-Orthogonal Sharing Mode (NOSM) [11]. But, the matching problem was the first thing needed to be solved for the EH-powered D2D communication underlaying cellular spectrum resources, and was ignored in the above researches [6], [8]–[10]. Therefore, we investigate the spectrum resource matching problem and the power control problem with joint consideration of the available energy state and the channel condition under a general cellular network. In the cellular network, D2D pairs are powered by EH technique, and are supposed to share the spectrum resource of CUs under NOSM.

The most related researches about our works are [12], [13]. Authors of [12] studied a downlink resource reuse system in the presence of multiple CUs and multiple underlay D2D links which were capable of harvesting energy from the surroundings. Under the circumstance that each D2D link can reuse the channel resource of one CU, they formulated a sum-rate maximization problem for D2D communication links, while protecting the cellular transmission rate requirement. But, the optimization of the whole network performance, and the mode of multiple D2D links multiplexing spectrum resource of one CU were not considered. In [13], energy cost minimization work was studied with QoS guarantees of both CU and DU, and two kinds of resource allocation algorithms were proposed for the minimization work based on the static or dynamic spectrum resource respectively.

The above two spectrum allocation schemes were the same as the matching schemes of the traditional D2D communications, which were mainly achieved based on the channel conditions between users, and ignored the influence of energy state. Thus, how to design an efficient resource allocation scheme with joint consideration of Channel State Information (CSI) and Energy State Information (ESI) for the EH-powered D2D Communication underlaying Cellular Networks (EH-DCCN) is a significant research work. As far as we know this work is an open research issue that has not been studied in the EH-DCCN.

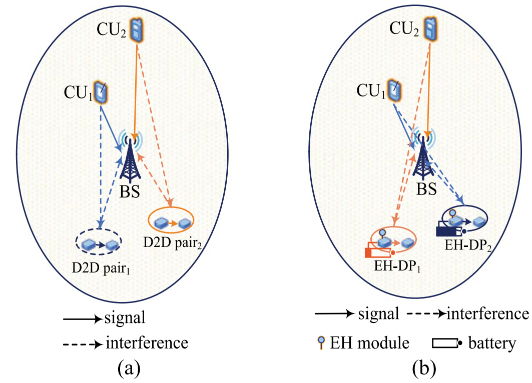

Fig. 1. The influence of available energy on optimal matching. (a) classical D2D communication. (b) EH-powered D2D communication.

B. Motivation

As illustrated by Fig. 1, we will take a single cellular network with two CUs and two D2D pairs as a simple example to elaborate our key motivation. In practice, D2D communication can exploit both uplink and downlink resources of a cellular system to transmit data. However, D2D communications using uplink resources only cause interference at the Base Station (BS), which generally has stronger processing abilities than CUs [14]–[16]. And meanwhile, uplink interference to D2D communications from CU is much lower than downlink interference from BS [17], [18]. Therefore, uplink reusing mode will be more energy efficient than downlink reusing mode for EH-powered D2D communications. Hence, we assume that D2D pairs only can reuse the uplink spectrum resources occupied by CUs to accomplish their local transmission. Furthermore, for brevity, let us consider the situation where each D2D pair can multiplex spectrum resource of one CU. In this paper, multiplex and reuse both represent the D2D pairs can use the same spectrum resource of CUs to transmit their local data under the NOSM. To maximize system transmission rate, under the classical D2D communication of Fig. 1(a), the optimal matching scheme is to allocate the proper channel resource of CUs for D2D pairs with consideration of the channel state, which is mainly influenced by the distance between users. Obviously, the optimal matching will let the D2D pair 1 and 2 reuse the spectrum resource of the CU 1 and 2, respectively. In this way can minimize the mutual interference between CU links and D2D links. However, under the EH-powered D2D communications scenario of Fig. 1(b), the optimal matching will be changed if the available energy of any of the two EH-powered D2D Pairs (EH-DPs) is not enough to support its transmission under stronger interference from CU links. For example, the available energy of the EH-DP 1 in battery is less than the EH-DP 2, and is not enough to support its transmission under interference from the CU 1. Thus, with joint consideration of the influence of the available energy and channel condition, the best matching decision is to let the

EH-DP 1 and 2 reuse the spectrum resource of the CU 2 and 1, respectively.

The matching problem under the classical D2D communications is studied and analyzed in many aspects, such as energy efficiency [19], [20], sum rate of D2D users [21], [22] and whole networks [23]. However, it is still an open issue under EH-powered D2D communications with joint consideration of the state of channel and power. Notably, the concepts of terms of energy and power are the same in this paper on the assumption that the length of a signal block is unit time [24]. Likewise, the corresponding power control strategies will also be changed. As we know, a typical power control problem is to find an optimal power allocation strategy that achieves the target utility functions [25]. Therefore, resource allocation problems in terms of the spectrum matching and power allocation will be studied in this paper.

C. Contributions

In this study, we investigate the resource allocation schemes in terms of the spectrum resource matching and the power allocation under a single EH-DCCN. In the EH-DCCN, D2D pairs powered by EH module are allowed to reuse the CUs' uplink spectrum resource to transmit their local data. Thus, the key contributions of this paper can be expressed as three aspects:

1) Firstly, this work is the first to consider the joint influence of the available energy and channel condition on the resource allocation schemes. Therefore, a sum transmission rate maximization problem in terms of the available energy and the QoS requirements of both CUs and EH-DPs is formulated. Moreover, multiple EH-DPs are permitted to reuse the same spectrum resource in the optimization problem;
2) Subsequently, two algorithms are proposed to solve the resource allocation optimization problem, which is a non-concave MINLP problem. On one hand, the theoretical lower bound on the original problem can be obtained by concave relaxation and Outer Approximation Algorithm (OAA); On the other hand, a suboptimal heuristic algorithm with low computational complexity, an Energy-aware Space Matching algorithm (ESM), is proposed;
3) As a consequence, we provide numerical results to assess the effectiveness of our proposed resource allocation strategy. Numerical simulation results indicate our considered resource allocation strategy is more effective than the strategy only based on CSI under the EH-DCCN. Moreover, the ESM can obtain approximate optimal theoretical performance of the lower bound under the scenarios with higher ratio of CU and EH-DP numbers. Furthermore, simulation results also give some insights to deploy the EH-DCCN by investigating the characteristics of the network.

The remainder of this paper is organized as follows. In Section II, we describe the system and energy harvesting model, and formulate the optimization problem. In section III, the algorithm of theoretical lower bound on the original problem, and the suboptimal heuristic algorithm ESM are described in detail. The numerical results are demonstrated and discussed in section IV. In section V, we draw a conclusion.

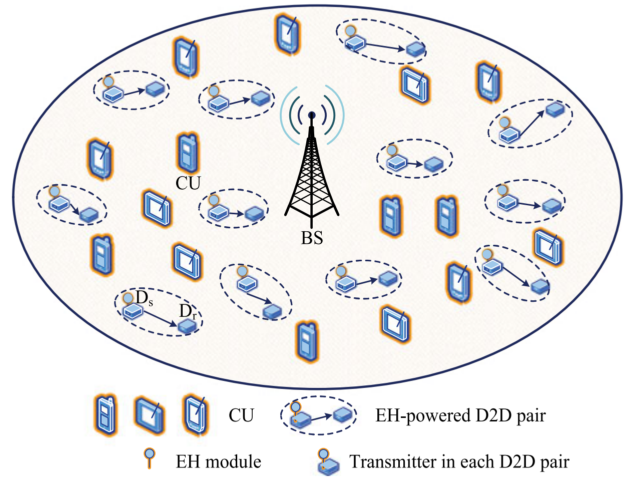

Fig. 2. System model of the EH-powered D2D communication underlaying cellular network.

II. Network Model and Problem Statement

In this section, we first depict the system components of the EH-powered D2D communication underlaying cellular networks. Then, we introduce the energy harvesting model. Finally, we describe and analyze our mathematical problem.

A. Scenario, Node and Transmission Model

We consider a single cellular network scenario which is illustrated by Fig. 2. A BS is located in the centre of the cell with radius R, while N_C CUs and N_D D2D pairs are uniformly distributed over the cell area. Suppose that the whole system operates in a time-slotted fashion, and all users have one antenna. Therefore, as the same assumption in [26], [27], the transmitter and the receiver of each D2D pair are supposed to be fixed during one time slot, which means the transmission mode is one-way. It is important to note that transmitters and receivers can be different in each time slot. Hence, in each time slot, the transmitter of each EH-DP is powered by an EH module, and equips a battery to store the harvested energy. At this time, the power of the D2D receiver node is not considered due to the low-power property of decode process. Let us assume that B represents BS, c_i $(i \in \{1, 2, \ldots, N_C\})$ is one CU in the CU set of Φ_C $(|\Phi_C| = N_C)$, and $d_j (j \in \{1, 2, \ldots, N_D\})$ is a pair of D2D users in the EH-DP set of Φ_D $(|\Phi_D| = N_D)$.

In this scenario, a higher frequency reuse factor is considered so that the intra-cell interference is not needed to be considered. In this system, there are N_C available orthogonal channels for CUs, and each of them has a bandwidth of B_W. At the same time, we assume that D2D links only can multiplex the uplink spectrum resource of CUs to accomplish their local data transmission. The traffic model of CU and D2D links is full buffer, meaning that there is always data to be sent at transmitting nodes in each time slot.

At each time slot, the binary indicator parameter $X = \left\{x_{c_i,d_j}\right\}, \left(x_{c_i,d_j} \in \{0,1\}\right)$ is defined to represent whether the d_j-th EH-DP reuses the uplink spectrum resource of the c_i-th CU. We suppose that 1 denotes "reuse", and 0 denotes "not reuse". In addition, the system assumes that each EH-DP is permitted to reuse no more than one CU's spectrum resource, and the spectrum resource of each CU is allowed to contain at most m EH-DPs. Thus, the above two assumptions can be expressed as follows:

$$\sum_{c_i} x_{c_i,d_j} \leq 1, (\forall d_j \in \Phi_D) \tag{1}$$

$$\sum_{d_j} x_{c_i,d_j} \leq m, (\forall c_i \in \Phi_C). \tag{2}$$

Based on the above analysis, the signal to interference plus noise ratio (SINR) of the c_i-th CU and the d_j-th D2D pair can be presented as follows:

$$R_{c_i} = \frac{p_{c_i} g_{c_i B}}{n_0 + \sum_{d_j} x_{c_i,d_j} p_{d_j} g_{d_j B}}, \tag{3}$$

$$R_{d_j} = \frac{p_{d_j} g_{d_j}}{n_0 + p_{c_i} g_{c_i d_j} + \sum_{\substack{d_k \neq d_j \\ d_k \in \Phi_D}} x_{c_i,d_k} p_{d_k} g_{d_k d_j}}, \tag{4}$$

where p_{c_i} and p_{d_j} are the transmission power of the c_i-th CU and the d_j-th EH-DP in a time slot, respectively. x_{c_i,d_j} $(c_i \in \Phi_C, d_j \in \Phi_D)$ is the multiplex indicator parameter. n_0 is the noise power, which equals to $B_W \cdot \rho_n$, where B_W is the uplink channel bandwidth and ρ_n is the density of noise. $g_{u_1u_2}$ $(u_1, u_2 \in \{B, \Phi_C, \Phi_D\})$, denotes the channel gain between transmitting node u_1 and receiving node u_2, which accounts for the path loss and Rayleigh fading and is expressed as

$$g_{u_1u_2} = L_{u_1u_2}^{-\alpha} \cdot |h_{u_1u_2}|, \tag{5}$$

where $L_{u_1u_2}$ is the distance between u_1 and u_2. α is the path-loss exponent between u_1 and u_2. $h_{u_1u_2} \sim \mathcal{CN}(0,1)$ is modeled as zero-mean complex Gaussian random variables with unit variance, characterizing the Rayleigh fading.

B. Energy Model

In this scenario, each EH-DP uses the harvested energy to transmit their local data. For the d_j-th EH-DP, $E_{d_j}^t$ units of energy can be harvested in the t-th time slot where $E_{d_j}^t \geq 0$. $\{E_{d_j}^1, E_{d_j}^2, \ldots, E_{d_j}^t, \ldots, E_{d_j}^T\}$ is the time sequence of harvested energy in T time slots. $E_{d_j}^t$ is also an i.i.d. sequence with Compound Poisson distribution: $E_{d_j}^t = \sum_{n=1}^{N(t)} U_{d_j}^n$ [28], where $N(t)$, the number of energy packets arriving at the time slot t, is assumed to be a homogeneous Poisson process with intensity λ_{d_j}. $U_{d_j}^n$ is the size of the n-th energy packet in $N(t)$. In addition, the λ_{d_j} and $U_{d_j}^n$ are called as EH efficiency of the d_j-th EH-DP.

Let $B_{d_j}^t$ depicts the amount of available energy in the battery for transmission at the time slot t of the d_j. The transmitted power $p_{d_j}^t$ is constrained by the available energy $B_{d_j}^t$ in the battery:

$$p_{d_j}^t \leq B_{d_j}^t, \left(B_{d_j}^t = B_{d_j}^{t-1} - p_{d_j}^{t-1} + E_{d_j}^{t-1}\right).$$

We assume that the energy are only for communication purposes. Existing energy in the battery can be retrieved without any loss and the battery capacity is large enough so that every quanta of incoming energy can be stored in the battery. This assumption is practically valid for the current circumstance of the technology in which batteries have very large capacities compared to the efficiency of harvested energy flow [29]. Besides, it is assumed that the CSI of all the involved links, and the ESI of all EH-DPs in each time slot are acquired by the BS so that the BS is capable of controlling the resource allocation.

C. Mathematic Model

This research investigates the optimal matching and the power allocation problems between CUs and EH-DPs in each time slot by studying the throughput maximization problem as **P1** shows:

$$\mathbf{P1}: \max_{X,P_C,P_D} \; R_{sum}(X, P_C, P_D), \tag{6a}$$

$$\text{s.t.} \quad \log(1 + R_{c_i}) \geq r_{c_i}^{th}, (\forall c_i \in \Phi_C), \tag{6b}$$

$$\log\left(1 + R_{d_j}\right) \geq r_{d_j}^{th}, (\forall d_j \in \Phi_D), \tag{6c}$$

$$0 \leq p_{c_i} \leq P_{c_i}^{\max}, \tag{6d}$$

$$0 \leq p_{d_j} \leq \min\left\{P_{d_j}^{\max}, B_{d_j}\right\}, \tag{6e}$$

$$\sum_{c_i} x_{c_i,d_j} \leq 1, (\forall d_j \in \Phi_D), \tag{6f}$$

$$\sum_{d_j} x_{c_i,d_j} \leq m, (\forall c_i \in \Phi_C), \tag{6g}$$

$$x_{c_i,d_j} \in \{0,1\}, \tag{6h}$$

where R_{sum} is the sum Shannon capacity of whole users including CUs and EH-DPs, which can be expressed as follow:

$$R_{sum}(X, P_C, P_D) = \sum_{c_i=1}^{N_C} \log(1 + R_{c_i}) + \sum_{c_i=1}^{N_C} \sum_{d_j=1}^{N_D} x_{c_i,d_j} \log\left(1 + R_{d_j}\right). \tag{7}$$

R_{c_i} and R_{d_j} are the SINR of c_i-th CU and d_j-th EH-DP, which are represented by equation (3) and (4) in detail, respectively. $X = \{x_{c_i,d_j}, (c_i \in \Phi_C, d_j \in \Phi_D)\}$ is the multiplex indicator parameter set. $P_C = \{p_{c_i}\}$ and $P_D = \{p_{d_j}\}$ are the sets of transmission power of CUs and EH-DPs, respectively. The (6b) and (6c) mean the transmission rate of the c_i-th CU and the d_j-th EH-DP should attain the minimum transmission rate threshold $r_{c_i}^{th}$ and $r_{d_j}^{th}$, respectively. At the same time, the (6d) and (6e) represent the maximal transmit power of the c_i and the d_j must lower than the available energy, respectively. Equation (6f) denotes each EH-DP can only reuse the uplink spectrum resource of one CU, and (6g) demonstrates the uplink spectrum resource of one CU can be multiplexed by at most m EH-DPs.

Throughout the text, logarithm expressed without a base, i.e., $log()$, refers to the natural logarithm $log_e()$.

D. Problem Analysis

With respect to **P1**, the solutions include the spectrum matching and the power allocation between CUs and EH-DPs based on the available energy and channel condition. Obviously, the spectrum matching problem for multiple EH-DPs under the constraints of the available energy and interference is a typical non-linear binary integer programming problem in each time slot. Moreover, the optimization problem will be a non-concave mixed integer non-linear programming problem (MINLP) [30], [31] with joint consideration of the power allocation scheme. It is so difficult and complex to find the optimal solutions about X, P_C, and P_D. Thus, we design two kinds of algorithms to solve the maximization problem. By consideration of the properties of the original problem, the first one is a tighten lower bound approximation approach and then solved by Outer Approximation Algorithm (OAA). But the computational complexity of the above approach can not satisfy the scheduling period of milliseconds in LTE systems although OAA can obtain an optimal tight lower-bound solution. Thus, we propose an Energy-aware Space Matching algorithm (ESM) with fast matching property and then determine the power allocation. In the next section, the two algorithms will be explained exactly.

III. Algorithms Design

In this section, two algorithms are explained at first, and the computational complexity of the two algorithms is elaborated in the later.

A. Outer Approximation Algorithm

Our approach considers a relaxation of the non-concave function (6) to solve this problem. In order to obtain the tight lower concave bound of the original problem, there are two important steps that should be implemented. First of all, we use the inequality (8) to obtain the lower bound of the original problem. In addition, this approximation is proved to be tight and have low computational complexity in [32], [33].

$$\alpha \log z_0 + \beta \le \log(1+z_0) \begin{cases} \alpha = \dfrac{z_0}{1+z_0}, \\ \beta = \log(1+z_0) - \alpha \log z_0. \end{cases} \tag{8}$$

Therefore, the tight lower bound of the non-concave problem **P1** can be rewritten by (8) as follows:

$$\max_{X, P_C, P_D} \sum_{c_i=1}^{N_C} \left(\alpha_{c_i} \log R_{c_i} + \beta_{c_i}\right) + \sum_{c_i=1}^{N_C} \sum_{d_j=1}^{N_D} x_{c_i,d_j} \left(\alpha_{d_j} \log R_{d_j} + \beta_{d_j}\right), \tag{9a}$$

$$\text{s.t.} \quad \alpha_{c_i} \log R_{c_i} + \beta_{c_i} \ge r_{c_i}^{th}, (\forall c_i \in \Phi_C), \tag{9b}$$

$$\alpha_{d_j} \log R_{d_j} + \beta_{d_j} \ge r_{d_j}^{th}, (\forall d_j \in \Phi_D), \tag{9c}$$

$$(6d) \sim (6h). \tag{9d}$$

Secondly, variables equality substitution of $p_{c_i} = e^{\tilde{p}_{c_i}}, p_{d_j} = e^{\tilde{p}_{d_j}}$ is implemented to obtain concavity of the original problem based on the first step. Therefore, the original problem **P1** can be expressed as:

$$\max_{X, \tilde{P}_C, \tilde{P}_D} f_{OA}(X, \tilde{P}_C, \tilde{P}_D) = \sum_{c_i=1}^{N_C} \tilde{f}_{c_i}\left(X, \tilde{p}_{c_i}, \tilde{P}_D\right) + \sum_{c_i=1}^{N_C} \sum_{d_j=1}^{N_D} x_{c_i,d_j} \tilde{f}_{d_j}\left(X, \tilde{P}_C, \tilde{P}_D\right), \tag{10a}$$

$$\text{s.t.} \quad \tilde{f}_{c_i}\left(X, \tilde{p}_{c_i}, \tilde{P}_D\right) \ge r_{c_i}^{th}, \tag{10b}$$

$$\tilde{f}_{d_j}\left(X, \tilde{P}_C, \tilde{P}_D\right) \ge r_{d_j}^{th}, \tag{10c}$$

$$\tilde{p}_{c_i} \le \log P_{c_i}^{\max}, \tag{10d}$$

$$\tilde{p}_{d_j} \le \min\left\{\log P_{d_j}^{\max}, \log B_{d_j}\right\}, \tag{10e}$$

$$(6f) \sim (6h), \tag{10f}$$

where $\tilde{f}_{c_i}(X, \tilde{p}_{c_i}, \tilde{P}_D)$ and $\tilde{f}_{d_j}(X, \tilde{P}_C, \tilde{P}_D)$ are described by (11) and (12), respectively. $\tilde{P}_C = \{\tilde{p}_{c_i}\} = \{\log(p_{c_i})\}$ and $\tilde{P}_D = \{\tilde{p}_{d_j}\} = \{\log(p_{d_j})\}$. The above maximization problem can easily be proved as a concave MINLP which satisfies the following propositions:

Proposition 1: In problem (10), $\tilde{P}_C$ and $\tilde{P}_D$ are nonempty, convex set; The objective function (10a), constraints (10b), (10c), (10d), and (10e) can be easily proofed to be concave by the convexity of *log-exp-sum*, for fixed values of X.

Proposition 2: The objective function (10a) and constraints (10b), (10c) are first order continuous differentiable.

Proposition 3: A constraint qualification holds at the solution of each concave nonlinear continuous sub-problem obtained by fixing the values of X.

Proposition 4: The concave nonlinear programming problem (concave NLP) obtained by fixing X can be solved by convex programming algorithms exactly.

$$\tilde{f}_{c_i}\left(X, \tilde{p}_{c_i}, \tilde{P}_D\right) = \alpha_{c_i} \log\left(g_{c_i B}\right) + \alpha_{c_i} \tilde{p}_{c_i} - \alpha_{c_i} \log\left(\sum_{d_j} x_{c_i,d_j} \exp\left(\tilde{p}_{d_j}\right) g_{d_j B} + n_0\right) + \beta_{c_i}. \tag{11}$$

$$\tilde{f}_{d_j}\left(X, \tilde{P}_C, \tilde{P}_D\right) = \alpha_{d_j} \log\left(g_{d_j}\right) + \alpha_{d_j} \tilde{p}_{d_j} - \alpha_{d_j} \log \times \left(\sum_{\substack{d_k \in \Phi_D \\ d_k \ne d_j}} x_{c_i,d_k} \exp\left(\tilde{p}_{d_k}\right) g_{d_k d_j} + \exp\left(\tilde{p}_{c_i}\right) g_{c_i d_j} + n_0\right) + \beta_{c_j}. \tag{12}$$

The concave MINLP (10) can be easily transformed into a convex MINLP minimization problem. And, the Outer Approximation Algorithm (OAA) [34], [35] is an effective way to solve this kind of convex MINLP problems by an iterative process. In the OAA, a convex MINLP problem is decoupled into a convex NLP primal problem (which fixes the integer variables) and an MILP master problem. The convex NLP primal problem optimizes the continuous variables and provides an upper bound to the convex MINLP solution, while the MILP master problem has the role of predicting a new lower bound for the convex MINLP solution, as well as a new integer variable for each iteration. The OAA uses sequence of non-increasing upper and non-decreasing lower bounds for the convex MINLP problem that satisfies the propositions 1–4. The OAA converges in a finite number of iterations with ε-convergence capability [36]. The sequence of the upper and lower bounds are obtained by solving the primal and master problem, respectively. Therefore, at the k-th iteration of the OAA, let the values of integer variable be fixed as $\widetilde{X}_{CD}^{k}$, the primal problem of (10) can be expressed as:

$$\min_{\widetilde{P}_C,\widetilde{P}_D} -f_{OA}\left(\widetilde{X}_{CD}^{k},\widetilde{P}_C,\widetilde{P}_D\right), \tag{13a}$$

$$\text{s.t.}\quad \widetilde{f}_{c_i}\left(\widetilde{X}_{CD}^{k},\widetilde{p}_{c_i},\widetilde{P}_D\right)\geq r_{c_i}^{th}, \tag{13b}$$

$$\widetilde{f}_{d_j}\left(\widetilde{X}_{CD}^{k},\widetilde{P}_C,\widetilde{P}_D\right)\geq r_{d_j}^{th}, \tag{13c}$$

$$(10d)\sim(10e). \tag{13d}$$

Solution of the primal problem will give the $\widetilde{P}_C^k,\widetilde{P}_D^k$ at the k-th iteration that will be used for the master problem of (10) as follows:

$$\min_{X}\left(\min_{\widetilde{P}_C,\widetilde{P}_D} -f_{OA}\left(\widetilde{X}_{CD}^{k},\widetilde{P}_C,\widetilde{P}_D\right)\right), \tag{14a}$$

$$\text{s.t.}\quad (13b)\sim(13d),(6f)\sim(6h). \tag{14b}$$

The problem (14) is the projection of (10) on X space. Since a constraint qualification holds at the solution of the primal problem (13) for every fixed $\widetilde{X}_{CD}^{k}$, the projection problem has the same solution as the problem below:

$$\underset{\left\{Z,X,\widetilde{P}_C,\widetilde{P}_D\right\}}{\text{minimize}}\quad Z, \tag{15a}$$

$$\text{s.t.}\quad -f_{OA}\left(\widetilde{X}_{CD}^{k},\widetilde{P}_C^k,\widetilde{P}_D^k\right)-\nabla f_{OA}\left(\widetilde{X},\widetilde{P}_C,\widetilde{P}_D\right)\times\begin{pmatrix}\widetilde{X}-\widetilde{X}_{CD}^{k}\\ \widetilde{P}_C-\widetilde{P}_C^k\\ \widetilde{P}_D-\widetilde{P}_D^k\end{pmatrix}-Z\leq 0, \tag{15b}$$

$$r_{c_i}^{th}-\widetilde{f}_{c_i}\left(\widetilde{X}_{CD}^{k},\widetilde{p}_{c_i}^k,\widetilde{P}_D^k\right)-\nabla\widetilde{f}_{c_i}\left(\widetilde{X}_{CD}^{k},\widetilde{p}_{c_i}^k,\widetilde{P}_D^k\right)\times\begin{pmatrix}\widetilde{X}-\widetilde{X}_{CD}^{k}\\ \widetilde{p}_{c_i}-\widetilde{p}_{c_i}^k\\ \widetilde{P}_D-\widetilde{P}_D^k\end{pmatrix}\leq 0, \tag{15c}$$

$$r_{d_j}^{th}-\widetilde{f}_{d_j}\left(\widetilde{X}_{CD}^{k},\widetilde{P}_C^k,\widetilde{P}_D^k\right)-\nabla\widetilde{f}_{d_j}\left(\widetilde{X}_{CD}^{k},\widetilde{P}_C^k,\widetilde{P}_D^k\right)\times\begin{pmatrix}\widetilde{X}-\widetilde{X}_{CD}^{k}\\ \widetilde{P}_C-\widetilde{P}_C^k\\ \widetilde{P}_D-\widetilde{P}_D^k\end{pmatrix}\leq 0, \tag{15d}$$

$$(10d)\sim(10e),(6f)\sim(6h). \tag{15e}$$

Algorithm 1: OAA.

Initialization: $\widetilde{X}_{CD}^{1}$;$k=1$;$\varepsilon=10^{-2}$;
Step 1: Transform the original problem **P1** into a convex MINLP problem as (10) shows according to the inequality (8) and the equality substitutions of $p_{c_i}=e^{\widetilde{p}_{c_i}}, p_{d_j}=e^{\widetilde{p}_{d_j}}$;
Step 2: Solve the NLP subproblem (15) of the convex MINLP (10) with the fixed $\widetilde{X}_{CD}^{k}$, and obtain the $(\widetilde{P}_C^k,\widetilde{P}_D^k)$ and an upper bound by $R_{sum}^{up}=R_{sum}(\widetilde{X}_{CD}^{k},\exp(\widetilde{P}_C^k),\exp(\widetilde{P}_D^k))$;
Step 3: Solve the MILP subproblem (15) of the convex MINLP (10), and obtain the $(\widetilde{X}_{CD}^{k^*},\widetilde{P}_C^{k^*},\widetilde{P}_D^{k^*})$ and a lower bound by $R_{sum}^{low}=R_{sum}(\widetilde{X}_{CD}^{k^*},\exp(\widetilde{P}_C^{k^*}),\exp(\widetilde{P}_D^{k^*}))$;
Step 4: Let the $\widetilde{X}_{CD}^{k+1}=\widetilde{X}_{CD}^{k^*}$ and the $k=k+1$;
Step 5: Repeat the step from 2 to 4 until the $R_{sum}^{up}-R_{sum}^{low}\leq\varepsilon$;
Update: R_{sum}^{OAA} by (7):
$R_{sum}^{OAA}=R_{sum}(\widetilde{X}_{CD}^{k},\exp\left(\widetilde{P}_C^k),\exp(\widetilde{P}_D^k\right))$.

The primal problem gives the upper bound and the master problem will give the lower bound for problem (10). The solution of the master problem provides the information for the next set of the integer variables $\widetilde{X}_{CD}^{k+1}$. As the iteration proceeds, these two bounds come close to each other. The algorithm will terminate when the difference between the two bounds is less than ε. A pseudo code for the OAA is given in Algorithm 1.

The OAA has a higher computational complexity even though it can obtain the theoretical lower bound on the original problem. The complexity of the OAA is one of key obstacles to be implemented in LTE system which requires the scheduling period in milliseconds. Thus, we propose a heuristic algorithm, Energy-aware Space Matching algorithm (ESM), which has fast matching property for CUs and EH-DPs.

B. Energy-Aware Space Matching Algorithm

Energy-aware Space Matching (ESM) algorithm solves the maximization problem **P1** by decomposing the problem into two steps. In the first step, the ESM implements a spectrum matching scheme to obtain the multiplex indicator parameter X; In the second step, the power allocation scheme is solved based on the first step so as to obtain the power variable sets P_C and P_D.

The first step, ESM should determine the spectrum matching indicator parameter X. As we all know, due to the fading characteristic of wireless communications, one simplest and fastest way to determine the matching parameter is based on distance constraint. But, how to set the distance and define the distance matching rules with joint consideration of available energy state and channel condition is the most important thing. In our model, according to the available power and the transmission rate constraints, the distance between CU c_i and EH-DP d_j must satisfy the following restraint if they can be matched:

$$\left|L_{c_i d_j}\right| \geq \left(\frac{p_{d_j} \cdot \left|L_{d_j}\right|^{-\alpha} - n_0\, \hat{r}_{d_j}^{th}}{\hat{r}_{d_j}^{th} \cdot \hat{r}_{c_i}^{th} \left(p_{d_j} \cdot \left|L_{d_j B}\right|^{-\alpha} + n_0\right) \cdot \left|L_{c_i B}\right|^{\alpha}} \right)^{-1/\alpha}$$

$$\geq \left[\left(\frac{\left|L_{d_j}\right|^{-\alpha}}{\psi} \right) \left(1 - \frac{\phi \cdot \left|L_{d_j}\right|^{-\alpha} + n_0 \cdot \psi \cdot \hat{r}_{d_j}^{th}}{\psi \cdot \left|L_{d_j}\right|^{-\alpha} \cdot p_{d_j} + \phi \cdot \left|L_{d_j}\right|^{-\alpha}} \right) \right]^{-1/\alpha}$$

where ψ represents $\hat{r}_{d_j}^{th} \cdot \hat{r}_{c_i}^{th} \cdot |L_{d_j B}|^{-\alpha} \cdot |L_{c_i B}|^{\alpha}$, ϕ is $\hat{r}_{d_j}^{th} \cdot \hat{r}_{c_i}^{th} \cdot |L_{c_i B}|^{\alpha} \cdot n_0$. The relevant derivation can be seen in Appendix A. Obviously, the value of $L_{c_i d_j}$ is proportional to $L_{c_i B}$ and inversely proportional to $L_{d_j B}$ and p_{d_j}. Calculating the relevant minimum required distance for all EH-DPs is a time-consuming process. Hence, we consider to set a uniform standard. In order to let as many EH-DPs as possible access network, we must consider the worst case. According to the relationship of $L_{c_i d_j}$ between the other variables, the EH-DP $\tilde{d}(\tilde{d} \in \Phi_D)$, which owns the minimum available transmission power and the worst channel quality (minimum distance from base station), is chosen. Furthermore, the CU $\tilde{c}(\tilde{c} \in \Phi_C)$ which is farthest away from BS is chosen. Hence, we can obtain the following corollary:

Corollary 1: In order to ensure the matched CU and EH-DPs have a feasible power allocation solution, the distance d_{EH} must satisfy a minimum value:

$$d_{EH} = \left|L_{\tilde{c}\tilde{d}}\right| \geq \left(\frac{p_{\tilde{d}} \cdot \left|L_{\tilde{d}}\right|^{-\alpha} - n_0\, \hat{r}_{\tilde{d}}^{th}}{\hat{r}_{\tilde{d}}^{th} \cdot \hat{r}_{\tilde{c}}^{th} \left(p_{\tilde{d}} \cdot \left|L_{\tilde{d}B}\right|^{-\alpha} + n_0\right) \cdot \left|L_{\tilde{c}B}\right|^{\alpha}} \right)^{-1/\alpha}.$$

Proof: The proof of this corollary is provided in Appendix A.

The d_{EH} is the minimum requisite multiplex distance, which is decided with joint consideration of the available energy and channel conditions. To solve the spectrum matching scheme in a faster and simpler way, ESM divides the cell area into two parts: Central Part (CP) and Edge Part (EP) according to d_{EH}. EH-DPs in different parts {CP or EP} can randomly reuse the CUs in the opposite part {EP or CP} to ensure the minimum distance constraint. Therefore, as shown in Fig. 3, a cellular network with R radius is divided into six 60 degree sectors [37]. The six sectors are named as 1 to 6 in counterclockwise order from north to south. Each sector is grouped into two parts: Central Part (CP) and Edge Part (EP) by d_{EH}. Moreover, to ensure the next power allocation step has a feasible solution, there are two matching rules we should be complied with:

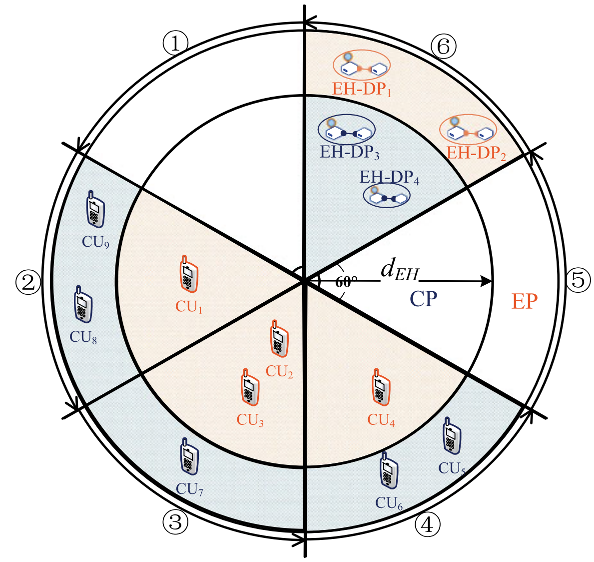

Fig. 3. Energy-aware Space Matching model.

1) EH-DPs in different parts {CP or EP} can randomly reuse the CUs in the opposite part {EP or CP} of the sectors which are opposite from each EH-DP sector. For example, as Fig. 3 illustrates, the EH-DPs in the EP (yellow) or CP (blue) part of the sixth sector can randomly multiplex the spectrum resource of CUs in the CP (yellow) or EP (blue) part of the opposite sectors {2,3,4} of the sixth sector;
2) EH-DPs in the same and adjacent sector can not reuse the same CU spectrum resource. As Fig. 3 shows, the spectrum resource of one CU reused by the EH-DP in the sixth sector can not be reused by EH-DPs in the sector 5 and 1 at the same time.

Based on the first rule, the division of CP and EP insures that the interference between CUs and EH-DPs is under control, which can effectively satisfy transmission rate requirements with the limitation of available energy. Likewise, the second rule makes sure that the mutual interference between EH-DPs is under control.

The second step, after obtaining the integer values of the multiplex indicator $\hat{X} = \{\hat{x}_{c_i,d_j}\}$, the proper power should be allocated between the matched CU and multiple EH-DPs to maximize the transmission rate of the whole network. Thus, the system transmission rate maximization problem can be divided into N_C subproblems due to the spectrum orthogonality of different CUs. Therefore, for any $c_i, (c_i \in \Phi_C)$, we have:

$$\max_{\{p_{c_i}, P_D\}} \log\left(1 + R_{c_i}\right) + \sum_{d_j=1}^{N_D} \hat{x}_{c_i,d_j} \log\left(1 + R_{d_j}\right), \quad (16a)$$

Algorithm 2: ESM.

for d_j = *1 to* N_D **do**
  for c_i = *1 to* N_C **do**
    if c_i *and* d_j *satisfy the two matching rules* **then**
      $\hat{x}_{c_i,d_j} = 1;$
      return;
    else
      $\hat{x}_{c_i,d_j} = 0;$
    end
  end
end
for c_i = *1 to* N_C **do**
  $\left\{\hat{p}_{c_i}, \hat{P}_D\right\} \leftarrow \arg \text{Problem}(17)$
end
Update: R_{sum}^{ESM} by (7):
$R_{sum}^{ESM} = R_{sum}\left(\hat{X}, \exp\left(\hat{P}_C\right), \exp\left(\hat{P}_D\right)\right).$

$$\text{s.t.} \quad \log\left(1 + R_{c_i}\right) \geq r_{c_i}^{th}, \tag{16b}$$

$$\log\left(1 + R_{d_j}\right) \geq r_{d_j}^{th}, \tag{16c}$$

$$(6d) \sim (6e), \tag{16d}$$

where EH-DP d_j belongs to Φ_D and reuses the spectrum resource of the CU c_i at the same time.

The above subproblem is also a non-concave maximization problem. But, we can obtain its theoretical lower bound by the approximation of (8) and the variables substitution of $p_{c_i} = e^{\tilde{p}_{c_i}}, p_{d_j} = e^{\tilde{p}_{d_j}}$:

$$\max_{\left\{\tilde{p}_c^i, \tilde{P}_D\right\}} \quad \tilde{f}_{c_i}\left(\hat{X}, \tilde{p}_{c_i}, \tilde{P}_D\right) + \sum_{d_j=1}^{N_D} \hat{x}_{c_i,d_j} \tilde{f}_{d_j}\left(\hat{X}, \tilde{P}_C, \tilde{P}_D\right), \tag{17a}$$

$$\text{s.t.} \quad \tilde{f}_{c_i}\left(\hat{X}, \tilde{p}_{c_i}, \tilde{P}_D\right) \geq r_{c_i}^{th}, \tag{17b}$$

$$\tilde{f}_{d_j}\left(\hat{X}, \tilde{P}_C, \tilde{P}_D\right) \geq r_{d_j}^{th}, \tag{17c}$$

$$(10d) \sim (10e). \tag{17d}$$

With the convexity of *log-exp-sum*, the problem (17) can be easily proved to be a concave maximization problem about relevant power parameters of CU and EH-DPs. The pseudo code of ESM can be detailedly expressed by Algorithm 2.

C. Complexity of OAA and ESM

Hijazi *et al.* [38] provided an example where outer approximation takes an exponential number of iterations about 2^n, in which n is the variables that need to be solved, and equals $N_C + N_D$ in this paper. In ESM, the system only needs to implement the proper matching method for each D2D, and solve N_C sub-problems of power allocation. Thus, the complexity of ESM can be expressed as $O(N_C \cdot N_D)$ in the worst case.

TABLE I
THE COMPARISON OF COMPLEXITY OF OAA AND ESM

	OAA	ESM
complexity	$O(2^{N_C+N_D})$	$O(N_C \cdot N_D)$

IV. SIMULATION RESULTS

In this section, the performance of the two proposed algorithms and the characteristics of the EH-DCCN are investigated in the performance of the average achievable system rate and the matching probability of EH-DPs. The matching probability of EH-DPs represents the ratio of the matched EH-DPs in N_D. To evaluate the effectiveness of the proposed algorithms, there are two comparison schemes should be described. The first one is the exhaustive searching method, which can enumerate all possible solutions, and thus attain an optimal solution. The second one is a graph-color method [39], which is one of typical resource allocation algorithms in classical D2D communication. Besides, all of the simulation model and algorithms are coded in the MATLAB.

However, the computational complexity of the exhaustive searching method increases exponentially with the number of the users [40]. Hence, it is difficult to implement the exhaustive searching method under large-scale scenario with large number of users. Therefore, we only compare the proposed algorithms OAA and ESM with the two comparison schemes under a small-scale scenario with 5 EH-DPs and different numbers of CUs (from 2 to 6). The scenario with the similar scale is set to validate the performance of algorithms proposed in [39], [41]. Moreover, under the large-scale scenario with 100 EH-DPs and different numbers of CUs (from 30 to 100), the performance of the two proposed algorithms is also evaluated by comparing with the graph-color method. Meanwhile, the characteristics of the network are investigated.

A. Simulation Setup

Above all, the detailed cellular network simulation settings should be illustrated. We consider a cellular network demonstrated by Fig. 2 with one Base Station (BS), N_C CUs and N_D EH-DPs. The BS is always located in the center of the cell, and the radius of the cellular network is 800 meters. The CUs and EH-DPs are randomly and uniformly distributed in the cell, and the position of all users is known by BS. Furthermore, the distance between receiver and sender of each EH-DP is randomly distributed in the range of 20 meters to 50 meters.

In order to study the effectiveness of the proposed algorithms and the characteristics of the EH-DCCN, we set up a small-scale scenario and a large-scale scenario. In each scenario, the energy packet arrival process for every EH-DP is supposed to be i.i.d random sample. This sample can be regarded as a statistic process obeying Poisson distribution with same parameter λ. Therefore, the energy packet arrival process, which is represented by $\lambda_{d_j} (\lambda_{d_j} = \lambda)$, is only considered as the variance of the EH efficiency. In the large-scale scenario, we define the ratio

TABLE II
EH-POWERED D2D SIMULATION SCENARIO PARAMETERS

Scenario settings		
	Description	Value
	BS position	at the center of the cell
	CUs and EH-DPs position	uniformly random distribution
	distance between sender and receiver of one EH-DP	random distribution in [20, 50] m
Simulation parameters settings		
Parameter	Description	Value
R	radius of the cell	800 m
N_C	sum number of CUs	large scale:[30:10:100] small scale:[2:1:6]
N_D	sum number of EH-DPs	large scale:100 small scale:5
B_W	uplink bandwidth of each orthogonal CU channel	180 KHz
ρ_n	thermal noise density	-174 dBm/Hz
α	path loss exponent for users	4
$P_{c_i}^{max}$	maximum transmission power constraints of CU	20 dBm
$P_{d_j}^{max}$	maximum transmission power constraints of d_i-th EH-DP	17 dBm
$N(t)$	the number of arriving energy packets in time slot t	Possion distribution with λ of [1:1:6]
$U_{d_i}^n$	average energy for each energy packet	0.0005 watt
m	the maximum reusable EH-DPs of one CU	3
$r_{c_i}^{th}$	minimum transmission rate threshold of CU	1 bps/Hz
$r_{d_j}^{th}$	minimum transmission rate threshold of d_i-th EH-DP	2 bps/Hz

of CU and EH-DP numbers as N_C/N_D. For each simulation scenario with different ratios or EH efficiencies, for example a scenario has a ratio of 0.5, we generate the corresponding random scenario about 100 times and average the performance of transmission rate and matching probability. All of the detailed network parameters used in this paper are demonstrated by Table II.

B. The Effectiveness of the Proposed Algorithms Under Small-Scale Scenario

Considering the high computational complexity of the exhaustive searching scheme for the scenarios with large number of users, a small-scale scenario is set to validate the effectiveness of the proposed algorithms. The small-scale scenario consists of 5 EH-DPs and different numbers of CUs (from 2 to 6). Under this small-scale scenario, the performances of the proposed algorithms and the comparison schemes in terms of average (avg.) achievable transmission rate and matching probability are demonstrated by Figs. 4 and 5, respectively. In this simulation, the EH efficiency λ is set as 2.

As shown in Figs. 4 and 5, the differences of sum rate and matching probability between OAA and the optimal exhaustive searching scheme are about 0.2 bit/s/Hz and 0.1, respectively.

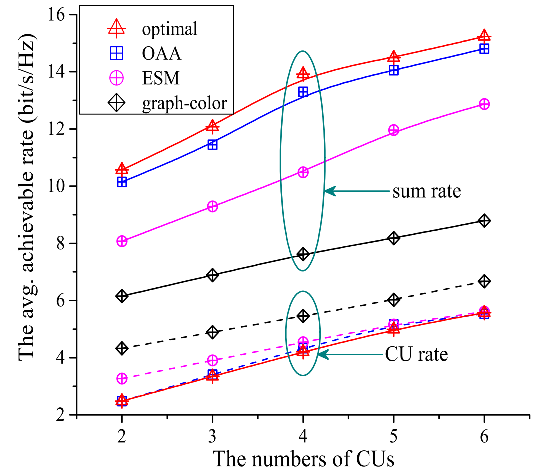

Fig. 4. The avg. achievable rate under the small-scale scenario.

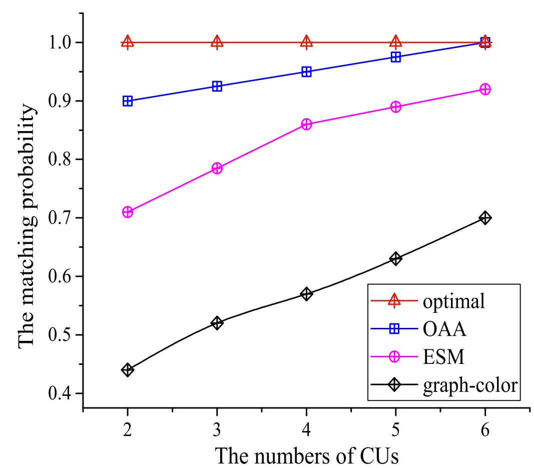

Fig. 5. The avg. matching probability under the small-scale scenario.

Hence, a vivid conclusion can be made that OAA can attain an approximate optimal sum rate and matching probability by comparing with the optimal exhaustive searching scheme. Simultaneously, although there is a gap about 2 bit/s/Hz in sum rate between the ESM and the optimal scheme, ESM also can obtain a suboptimal performance, while owning the lowest computational complexity and satisfying the transmission rate requirements of users.

Moreover, two principle reasons can explain the poorest performance of the graph-color method. Firstly, the graph-color method randomly allocates channel resource of CU based on the constructed graph and the interference negligible distance (INS) and SIR limited area (SLA). The INS is a fixed value and the SLA is only based on channel state but ignores the energy feature. Thus, the spectrum resource matching strategy will be invalid if the available energy of D2D pairs cannot achieve their transmission rate requirements under the corresponding interference. Secondly, the graph-color method tries its best to allocate proper D2D pairs for each CU, one after the other, which will lead to unbalanced distribution of resources. In other words, some CUs share their channels with multiple D2D pairs, but some CUs are not paired with any D2D links. Finally, the

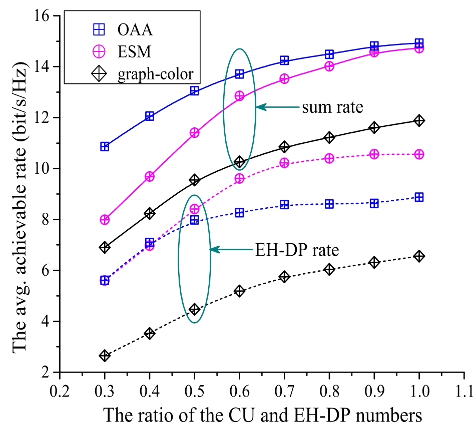

Fig. 6. The avg. achievable rate versus different ratios of CU and EH-DP numbers under large-scale scenario.

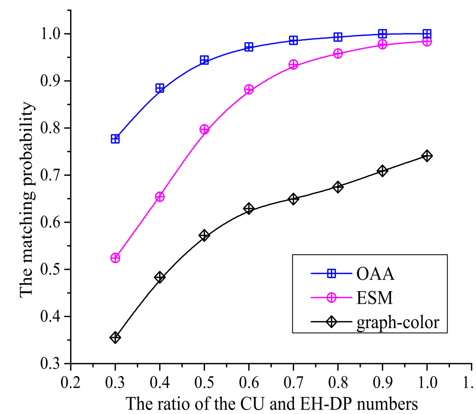

Fig. 7. The avg. matching probability versus different ratios of CU and EH-DP numbers under large-scale scenario.

unbalanced distribution of resources will result in large mutual interference among D2D links, and thus the sum transmission rate is not substantially improved.

Furthermore, the average CU rate in Fig. 4 shows the different characteristics of the above algorithms. Under the graph-color method, the CUs own the smallest interference from EH-DPs due to the unsuccessful matching, and thus CUs have the best transmission rate than other algorithms. On the contrary, the optimal exhaustive searching scheme and the OAA have the highest matching probability, which will result in that the CUs suffer the largest interference from EH-DPs. Hence, the transmission rate performance of CUs in optimal scheme and OAA is the lowest than others. Based on this, the transmission rate of the heuristic algorithm ESM is performed in the middle of all algorithms. Besides, when the node numbers of CUs are little, the number of EH-DPs reusing the same channel resource is higher. This phenomenon will result in the more interference to the CUs, and thus the avg. achievable transmission rate of CUs is smaller. Hence, the avg. achievable rate of CUs will increase with the raise of the number of CUs.

C. Simulation Results in Large-Scale Scenario

There are two principle purposes to design the large-scale scenario. The first one is to evaluate the performance of the proposed algorithms. The second one is to investigate the influence of different ratios on performance. The large-scale scenario is set with 100 EH-DPs and different numbers of CUs (from 30 to 100). In this simulation, the EH efficiency λ is also set as 2. The average achievable rate and the matching probability are illustrated in detail by Figs. 6 and 7, respectively.

There are three important phenomena can be seen in Figs. 6 and 7. The first one is that our proposed algorithms still outperform the performance of graph-color in terms of transmission rate and matching probability.

The second, the performance of ESM in sum rate gradually approaches to the optimal lower bound of OAA along with the increasing of the ratio. When the ratio is not less than 0.6, the difference of sum rate between the ESM and the OAA is less than 1 bit/s/Hz. The same phenomenon can be also reflected by the matching probability of EH-DPs in Fig. 7. The average matching probability of EH-DPs in the ESM is gradually increasing to the OAA, and closing to one hundred percentage as the ratio rises. It vividly implies that the ESM can obtain the approximate performance of the theoretical tight lower bound on the original problem under the scenarios with the balanced distribution between the CUs and EH-DPs. With low computational complexity, the ESM is more suitable for the scenarios with the large scale of users and a higher ratio.

Thirdly, as demonstrated by the average achievable rate of EH-DP in Fig. 6, the ESM and the OAA are concentrated on different aspects aiming at improving the system performance. In another word, the ESM is more concerned with the rate improvement of EH-DPs. On the contrary, the OAA pays more attention to the rate improvement of CUs.

The above phenomenon can be interpreted as follows:

The OAA can acquire the optimal lower bound of the original maximization problem by the iteration process. To obtain the maximal transmission rate, the OAA will let EH-DPs match the corresponding CU as many as possible under the interference constraints. On the contrary, the maximum number of EH-DPs reusing same CU in the ESM is less than the OAA in nature. The ESM scheme only can make each CU maintain at most two EH-DPs essentially. Hence, there will be more interference for each CU in the OAA than the ESM when the ratio is low. But the number of EH-DPs multiplexing one CU in the OAA exceeds that in the ESM. Hence, the system rate and the matching probability in the OAA are still better than the ESM. This explanation is also be proved in the simulation of the variation of the average system rate in Fig. 6. As we can see in this figure, due to the matching property of the ESM, the average sum rate of the ESM is lower than the OAA when the ratio is less than 0.6. This phenomenon also explains why the ESM gets poor performance under the scenarios with lower ratio of CU and EH-DP numbers.

D. The Influence of Different EH Efficiencies on Performance

Under the same large-scale scenarios of section IV-C, the impact of EH efficiency λ on performance is also investigated.

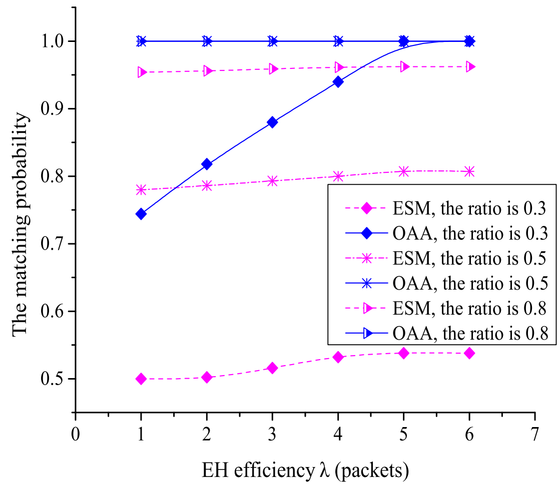

Fig. 8. The avg. matching probability VS. different EH efficiencies under large-scale scenario.

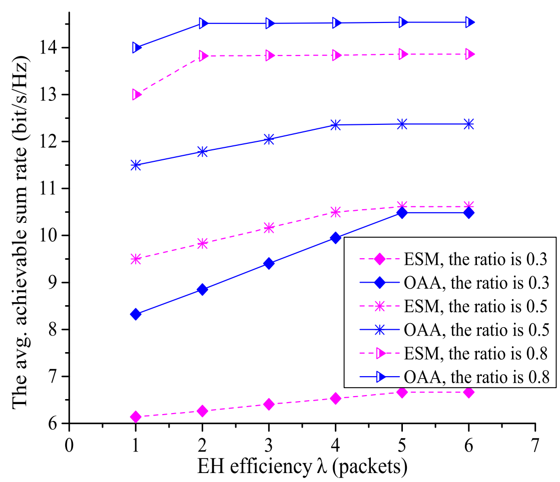

Fig. 9. The avg. achievable rate VS. different EH efficiencies under large-scale scenario.

As demonstrated by Figs. 8 and 9, the matching probability is gradually increasing with the rise of λ, especially under the scenarios with lower ratio such as under 0.3. This is because the EH-DPs' ability to tolerate interference is increasing as the harvested energy rises. So, more and more EH-DPs can multiplex the spectrum resource of one CU at the same time under the control of interference. Therefore, the sum transmission rate is also growing with the rise of EH efficiency. However, as illustrated by Figs. 8 and 9, the influence of the growth of harvested energy on performance in the ESM is not more instinct than the OAA. This phenomenon can be mainly explained by the reason that although the growth of energy can make EH-DPs possible to bear more interference, the matching rules in the ESM will not be changed. In other words, the maximum tolerable EH-DP numbers of one CU in the ESM will not be changed due to the space matching property. Thus, the performance of the ESM is more stable than the OAA. But, the performance of the ESM can approach the OAA under the scenarios with the large ratio such as up to 0.8.

In addition, we can get some crucial conclusions from the performance of OAA. Due to the maximum transmission power constraints, the rise of EH efficiency cannot always increase the system performance. From the simulation results, the matching probability is close to 1 when the EH efficiency reaches 5 and the ratio is 0.3. The more distinct phenomenon can be seen in sum rate as Fig. 9 shows. The system rate is not rising when the λ equals 5. Besides, when the ratio is 0.5 or 0.8, the OAA performs stably when EH efficiency λ reaches 4 or 2 in aspects of the matching probability and sum rate, respectively. Thus, we can conclude that the ratio of CU and EH-DP numbers must be above 0.8 when EH efficiency is 2, and ratio is 0.5 or 0.3 when EH efficiency is 4 or 5, respectively. This conclusion can give an insight needed for the central controller to deploy EH-powered D2D communication underlaying cellular networks.

V. Conclusion

In this paper, we study the resource allocation scheme for EH-powered D2D communication underlaying cellular networks. Unlike the conventional D2D communications, the achievable energy will become another significant issue that resource allocation schemes must be considered in the EH-powered D2D communication. Thus, we investigate a sum-rate maximization problem in terms of the available energy and the transmission rate requirement under a single cellular network. Due to the optimization problem being a non-concave MINLP, we obtain the optimal lower bound of the original problem by a concave approximation and OAA algorithm. At the same time, because of the high complexity of OAA, we propose a heuristic algorithm, which is named Energy-aware Space Matching (ESM) algorithm. ESM decomposes the original problem into the spectrum matching problem and the power allocation problem. And then, ESM firstly solves the spectrum matching problem, and then allocates the proper power for the matched CU and EH-DPs. The time complexity of OAA and ESM in the worst case are $O(2^{N_C+N_D})$ and $O(N_C \cdot N_D)$, respectively. Obviously, the ESM own a lower complexity than OAA.

In the simulation, different scenarios with different ratios and EH efficiencies are set to assess the effectiveness of the two algorithms and study the characteristics of the EH-powered D2D communication. From simulations, some vivid results can be obtained. First of all, simulation results imply that our considered resource allocation strategy is more effective than the strategy only based on channel state information under EH-DCCN. Secondly, the ESM algorithm with low computational complexity is more suitable for the scenarios with higher ratio than OAA. Finally, it is better to keep the ratio above 0.8 when EH efficiency of EH-DPs is low, and the EH efficiency of EH-DPs is up to 5 if the user density of EH-DPs is larger than CUs. This results can give some insights for the central controller to deploy EH-DCCN in the future.

Appendix
Proof of Corollary 1

According to the reusing rules of the ESM, the distance among EH-DPs reusing the same spectrum of one CU is enough far away from each other. Hence, the interference among EH-DPs can be approximately ignored. Based on this, the minimum reusing radius d_{EH} is approximately determined by the CU and the EH-DP reusing the same spectrum resource. Hence, according to the transmission rate requirement, the matched CU c_i and EH-DP d_j must satisfy the following constraints:

$$\begin{cases} \log\left(1+\frac{p_{c_i}\cdot\left|L_{c_iB}\right|^{-\alpha}}{n_0+p_{d_j}\cdot\left|L_{d_jB}\right|^{-\alpha}}\right)\ge r_{c_i}^{th}, \\ \log\left(1+\frac{p_{d_j}\cdot\left|L_{d_j}\right|^{-\alpha}}{n_0+p_{c_i}\cdot\left|L_{c_id_j}\right|^{-\alpha}}\right)\ge r_{d_j}^{th}. \end{cases}$$

It can be converted as follow when all variables are equal or larger than zero:

$$\begin{cases} \frac{p_{c_i}\cdot\left|L_{c_iB}\right|^{-\alpha}}{n_0+p_{d_j}\cdot\left|L_{d_jB}\right|^{-\alpha}}\ge \hat{r}{}_{c_i}^{th}, \\ \frac{p_{d_j}\cdot\left|L_{d_j}\right|^{-\alpha}}{n_0+p_{c_i}\cdot\left|L_{c_id_j}\right|^{-\alpha}}\ge \hat{r}{}_{d_j}^{th}, \end{cases}$$

where $\hat{r}{}_{c_i}^{th}=\exp(r_{c_i}^{th})-1, \hat{r}{}_{d_j}^{th}=\exp(r_{d_j}^{th})-1$. Thus, we can obtain the following inequality conditions:

$$\begin{cases} p_{c_i}\ge \hat{r}{}_{c_i}^{th}\left(p_{d_j}\cdot\left|L_{d_jB}\right|^{-\alpha}+n_0\right)\cdot\left|L_{c_iB}\right|^{\alpha}, \\ \left|L_{c_id_j}\right|\ge\left(\frac{p_{d_j}\cdot\left|L_{d_j}\right|^{-\alpha}-n_0\,\hat{r}{}_{d_j}^{th}}{\hat{r}{}_{d_j}^{th}\cdot p_{c_i}}\right)^{-1/\alpha}. \end{cases}$$

Put p_{c_i} into $\left|L_{c_id_j}\right|$:

$$\begin{aligned} \left|L_{c_id_j}\right| &\ge \left(\frac{p_{d_j}\cdot\left|L_{d_j}\right|^{-\alpha}-n_0\,\hat{r}{}_{d_j}^{th}}{\hat{r}{}_{d_j}^{th}\cdot\hat{r}{}_{c_i}^{th}\left(p_{d_j}\cdot\left|L_{d_jB}\right|^{-\alpha}+n_0\right)\cdot\left|L_{c_iB}\right|^{\alpha}}\right)^{-1/\alpha} \\ &\ge \left[\left(\frac{\left|L_{d_j}\right|^{-\alpha}}{\psi}\right)\left(1-\frac{\phi\cdot\left|L_{d_j}\right|^{-\alpha}+n_0\cdot\psi\cdot\hat{r}{}_{d_j}^{th}}{\psi\cdot\left|L_{d_j}\right|^{-\alpha}\cdot p_{d_j}+\phi\cdot\left|L_{d_j}\right|^{-\alpha}}\right)\right]^{-1/\alpha} \end{aligned}$$

where ψ represents $\hat{r}{}_{d_j}^{th}\cdot\hat{r}{}_{c_i}^{th}\cdot|L_{d_jB}|^{-\alpha}\cdot|L_{c_iB}|^{\alpha}$, ϕ is $\hat{r}{}_{d_j}^{th}\cdot\hat{r}{}_{c_i}^{th}\cdot|L_{c_iB}|^{\alpha}\cdot n_0$. As illustrated by the above inequality function, if the EH-DP d_j can reuse the CU c_i's spectrum resource to transmit, we can obtain the minimum reusing distance between the matched CU c_i and EH-DP d_j. Obviously, the value of $L_{c_id_j}$ is proportional to L_{c_iB} and inversely proportional to L_{d_jB} and p_{d_j}. In order to let as many EH-DPs as possible can multiplex CU's spectrum resource, we must consider the worst case. According to the relationship of $L_{c_id_j}$ between the other variables, the EH-DP $\tilde{d}(\tilde{d}\in\Phi_D)$, which owns the minimum available transmission power and the worst channel quality (minimum distance from base station), is chosen. Furthermore, the CU $\tilde{c}(\tilde{c}\in\Phi_C)$ which is farthest away from BS is chosen. Hence, the minimum matching radius d_{EH}, which ensures as many EH-DPs as possible can multiplex cellular spectrum resources, is shown as follow:

$$\begin{aligned} d_{EH} &= \left|L_{\tilde{c}\tilde{d}}\right| \\ &\ge \left(\frac{p_{\tilde{d}}\cdot\left|L_{\tilde{d}}\right|^{-\alpha}-n_0\,\hat{r}{}_{\tilde{d}}^{th}}{\hat{r}{}_{\tilde{d}}^{th}\cdot\hat{r}{}_{\tilde{c}}^{th}\left(p_{\tilde{d}}\cdot\left|L_{\tilde{d}B}\right|^{-\alpha}+n_0\right)\cdot\left|L_{\tilde{c}B}\right|^{\alpha}}\right)^{-1/\alpha}. \end{aligned}$$

Acknowledgment

The authors would sincerely thank the anonymous referees for their invaluable suggestions that have led to the present improved version of the original manuscript.

References

[1] X. Lin, J. Andrews, A. Ghosh, and R. Ratasuk, “An overview of 3GPP device-to-device proximity services,” *IEEE Commun. Mag.*, vol. 52, no. 4, pp. 40–48, Apr. 2014.

[2] F. Wang, Y. Li, Z. Wang, and Z. Yang, “Social-community-aware resource allocation for D2D communications underlaying cellular networks,” *IEEE Trans. Veh. Technol.*, vol. 65, no. 5, pp. 3628–3640, May 2016.

[3] N. K. Pratas and P. Popovski, “Underlay of low-rate machine-type D2D links on downlink cellular links,” in *Proc. IEEE Int. Conf. Commun. Workshops*, 2014, pp. 423–428.

[4] Z. Ding, S. M. Perlaza, I. Esnaola, and H. V. Poor, “Power allocation strategies in energy harvesting wireless cooperative networks,” *IEEE Trans. Wireless Commun.*, vol. 13, no. 2, pp. 846–860, Feb. 2014.

[5] V. Raghunathan, S. Ganeriwal, and M. Srivastava, “Emerging techniques for long lived wireless sensor networks,” *IEEE Commun. Mag.*, vol. 44, no. 4, pp. 108–114, Apr. 2006.

[6] A. H. Sakr and E. Hossain, “Cognitive and energy harvesting-based D2D communication in cellular networks: Stochastic geometry modeling and analysis,” *IEEE Trans. Commun.*, vol. 63, no. 5, pp. 1867–1880, May 2015.

[7] D. W. K. Ng and R. Schober, “Secure and green SWIPT in distributed antenna networks with limited backhaul capacity,” *IEEE Trans. Wireless Commun.*, vol. 14, no. 9, pp. 5082–5097, Sep. 2015.

[8] H. Yang, J. Lee, and T. Quek, “Heterogeneous cellular network with energy harvesting based D2D communication,” *IEEE Trans. Wireless Commun.*, vol. 15, no. 2, pp. 1406–1419, Feb. 2016.

[9] K. Tutuncuoglu and A. Yener, “Sum-rate optimal power policies for energy harvesting transmitters in an interference channel,” *J. Commun. Netw.*, vol. 14, no. 2, pp. 151–161, 2012.

[10] Z. Zhou, G. Ma, C. Xu, and Z. Chang, “A game-theoretical approach for green power allocation in energy-harvesting device-to-device communications,” in *Proc. IEEE Veh. Technol. Conf.*, 2016, pp. 1–5.

[11] H. Lu, Y. Wang, Y. Chen, and K. R. Liu, “Stable throughput region and admission control for device-to-device cellular coexisting networks,” *IEEE Trans. Wireless Commun.*, vol. 15, no. 4, pp. 2809–2824, Apr. 2016.

[12] S. Gupta, R. Zhang, and L. Hanzo, “Energy harvesting aided device-to-device communication underlaying the cellular downlink,” *IEEE Access*, vol. 5, pp. 1–10, Aug. 2016.

[13] J. Ding, L. Jiang, and C. He, “Dynamic spectrum allocation for energy harvesting-based underlaying D2D communication,” in *Proc. IEEE Veh. Technol. Conf.*, 2016, pp. 1–5.

[14] J. Wang, D. Zhu, C. Zhao, J. C. Li, and M. Lei, “Resource sharing of underlaying device-to-device and uplink cellular communications,” *IEEE Commun. Lett.*, vol. 17, no. 6, pp. 1148–1151, Jun. 2013.

[15] D. Feng, L. Lu, Y. Yuan-Wu, G. Y. Li, G. Feng, and S. Li, “Device-to-device communications underlaying cellular networks,” *IEEE Trans. Commun.*, vol. 61, no. 8, pp. 3541–3551, Aug. 2013.

[16] R. Liu, G. Yu, F. Qu, and Z. Zhang, “Device-to-device communications in unlicensed spectrum: Mode selection and resource allocation,” *IEEE Access*, vol. 4, pp. 4720–4729, Aug. 2016.

[17] W.-B. Yang, M. Souryal, and D. Griffith, “LTE uplink performance with interference from in-band device-to-device (D2D) communications,” in *Proc. IEEE Wireless Commun. Netw. Conf.*, 2015, pp. 669–674.

[18] F. Wang, C. Xu, L. Song, and Z. Han, “Energy-efficient resource allocation for device-to-device underlay communication,” *IEEE Trans. Wireless Commun.*, vol. 14, no. 4, pp. 2082–2092, Dec. 2015.

[19] H. Xu, W. Xu, Z. Yang, Y. Pan, J. Shi, and M. Chen, "Energy-efficient resource allocation in D2D underlaid cellular uplinks," *IEEE Commun. Lett.*, vol. 21, no. 3, pp. 560–563, Nov. 2016.

[20] Z. Zhou, K. Ota, M. Dong, and C. Xu, "Energy-efficient matching for resource allocation in D2D enabled cellular networks," *IEEE Trans. Veh. Technol.*, vol. 66, no. 6, pp. 5256–5258, Oct. 2016.

[21] D. Zhu, J. Wang, A. L. Swindlehurst, and C. Zhao, "Downlink resource reuse for device-to-device communications underlaying cellular networks," *IEEE Signal Process. Lett.*, vol. 21, no. 5, pp. 531–534, Feb. 2014.

[22] R. Yin, C. Zhong, G. Yu, Z. Zhang, K. K. Wong, and X. Chen, "Joint spectrum and power allocation for D2D communications underlaying cellular networks," *IEEE Trans. Veh. Technol.*, vol. 65, no. 4, pp. 2182–2195, Apr. 2016.

[23] G. Yu, L. Xu, D. Feng, R. Yin, G. Y. Li, and Y. Jiang, "Joint mode selection and resource allocation for device-to-device communications," *IEEE Trans. Commun.*, vol. 62, no. 11, pp. 3814–3824, Oct. 2014.

[24] T. Li, P. Fan, and K. B. Letaief, "Outage probability of energy harvesting relay-aided cooperative networks over Rayleigh fading channel," *IEEE Trans. Veh. Technol.*, vol. 65, no. 2, pp. 972–978, Feb. 2016.

[25] H. H. Kha, H. D. Tuan, and H. H. Nguyen, "Fast global optimal power allocation in wireless networks by local DC programming," *IEEE Trans. Wireless Commun.*, vol. 11, no. 2, pp. 510–515, Feb. 2012.

[26] N. Lee, X. Lin, J. G. Andrews, and R. W. Heath, "Power control for D2D underlaid cellular networks: Modeling, algorithms, and analysis," *IEEE J. Sel. Areas Commun.*, vol. 33, no. 1, pp. 1–13, Jan. 2015.

[27] Y. Li, M. C. Gursoy, and S. Velipasalar, "Joint mode selection and resource allocation for D2D communications under queueing constraints," in *Proc. IEEE Conf. Comput. Commun. Workshops*, 2016, pp. 490–495.

[28] M. P, "On optimal online policies in energy harvesting systems for compound poisson energy arrivals," in *Proc. IEEE Int. Symp. Inf. Theory*, 2012, pp. 960–964.

[29] V. Sharma, U. Mukherji, V. Joseph, and S. Gupta, "Optimal energy management policies for energy harvesting sensor nodes," *IEEE Trans. Wireless Commun.*, vol. 9, no. 4, pp. 1326–1336, Apr. 2010.

[30] J. Lee and S. Leyffer, *Mixed Integer Nonlinear Programming*, vol. 154. Berlin, Germany: Springer Science and Business Media, 2011.

[31] S. Burer and A. N. Letchford, "Non-convex mixed-integer nonlinear programming: A survey," *Surv. Oper. Res. Manage. Sci.*, vol. 17, no. 2, pp. 97–106, 2012.

[32] W. Zhao and S. Wang, "Low complexity power allocation for device-to-device communication underlaying cellular networks," in *Proc. IEEE Int. Conf. Commun.*, 2014, pp. 5532–5537.

[33] J. Papandriopoulos and J. S. Evans, "SCALE: A low-complexity distributed protocol for spectrum balancing in multiuser DSL networks," *IEEE Trans. Inf. Theory*, vol. 55, no. 8, pp. 3711–3724, Aug. 2009.

[34] C. DAmbrosio, "Application-oriented mixed integer non-linear programming," *4OR: A Quart. J. Oper. Res.*, vol. 8, no. 3, pp. 319–322, 2010.

[35] P. Belotti, C. Kirches, S. Leyffer, J. Linderoth, J. Luedtke, and A. Mahajan, "Mixed-integer nonlinear optimization," *Acta Numerica*, vol. 22, pp. 1–131, 2013.

[36] R. Fletcher and S. Leyffer, "Solving mixed integer nonlinear programs by outer approximation," *Math. Program.*, vol. 66, no. 1-3, pp. 327–349, 1994.

[37] S. Lohani, R. A. Loodaricheh, E. Hossain, and V. K. Bhargava, "On multiuser resource allocation in relay-based wireless-powered uplink cellular networks," *IEEE Trans. Wireless Commun.*, vol. 15, no. 3, pp. 1851–1865, Mar. 2016.

[38] H. Hijazi, P. Bonami, and A. Ouorou, "An outer-inner approximation for separable MINLPs," LIF, Faculté des Sciences de Luminy, Université de Marseille, Marseille, France, Tech. Rep, 2010.

[39] X. Cai, J. Zheng, and Y. Zhang, "A graph-coloring based resource allocation algorithm for D2D communication in cellular networks," in *Proc. IEEE Int. Conf. Commun.*, 2015, pp. 5429–5434.

[40] T. Jiang, W. Xiang, P. C. Richardson, J. Guo, and G. Zhu, "PAPR reduction of OFDM signals using partial transmit sequences with low computational complexity," *IEEE Trans. Broadcast.*, vol. 53, no. 3, pp. 719–724, Sep. 2007.

[41] R. Yin, G. Yu, H. Zhang, Z. Zhang, and G. Y. Li, "Pricing-based interference coordination for D2D communications in cellular networks," *IEEE Trans. Wireless Commun.*, vol. 14, no. 3, pp. 1519–1532, Mar. 2015.

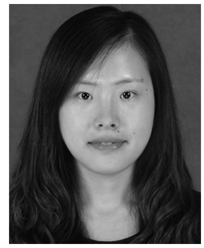

Ying Luo received the B.S. and M.S. degrees from the Department of Information Engineering, South West University of Science and Technology (SWUST), Mianyang, China, in 2012 and 2015, respectively. She is currently working toward the Ph.D. degree in information and communication engineering from the Department of Electronic Engineering and Information Science (EEIS), University of Science and Technology of China (USTC). Her research interests include the analysis of heterogeneous cellular networks.

Peilin Hong received the B.S. and M.S. degrees from the Department of Electronic Engineering and Information Science (EEIS), University of Science and Technology of China (USTC), Hefei, China, in 1983 and 1986, respectively. She is currently a Professor and an Advisor for Ph.D. candidates in the Department of EEIS, USTC. Her research interests include next-generation Internet, policy control, IP QoS, and information security. She has published 2 books and more than 150 academic papers in several journals and conference proceedings.

Ruolin Su received the B.S. degree from the Department of Communications Engineering, Harbin Institute of Technology, Harbin, China, in 2016. She is currently working toward the M.S. degree in the Department of Electronic Engineering and Information Science, University of Science and Technology of China. Her current research interest is resource allocation in device-to-device communication.

Kaiping Xue was born in 1980. He received the B.S. degree from the Department of Information Security, University of Science and Technology of China (USTC), Hefei, China, in 2003 and the Ph.D. degree from the Department of Electronic Engineering and Information Science (EEIS), USTC, in 2007. He is currently an Associate Professor in the Department of Information Security and Department of EEIS, USTC. His research interests include next-generation Internet, distributed networks, and network security.